

VIII. TUBE RESEARCH AND DEVELOPMENT

A. MAGNETRON DEVELOPMENT

Dr. S. T. Martin
A. G. Barrett

1. Testing and Design of High-Power 10.7-Cm Magnetrons

Assembly of MF-13B magnetron was discontinued after a leak developed at the window during a second attempt to braze the window assembly to the output section.

Magnetron MF-14B was assembled successfully with the structural and cathode changes described in the last Quarterly Progress Report and placed on the pumps. These structural and cathode changes included oversize cathode end shields, new end plate rings, and the addition of carbonyl process nickel powder to the cathode coating mixture in equal proportions with the carbonates. During the preliminary stages of bakeout a leak occurred in a cathode lead metal-ceramic seal while the temperature was 450°C. Efforts to patch the leak failed, and since the pressure was 1.2×10^{-5} mm Hg at 425°C, it was decided to continue baking by raising the temperature to 700°C in three steps, as an external atmosphere of very pure nitrogen was surrounding the tube. Hence the leak was not likely to affect the cathode.

Upon cooling the tube down after it baked for 19 hours at 700°C, we found it to be

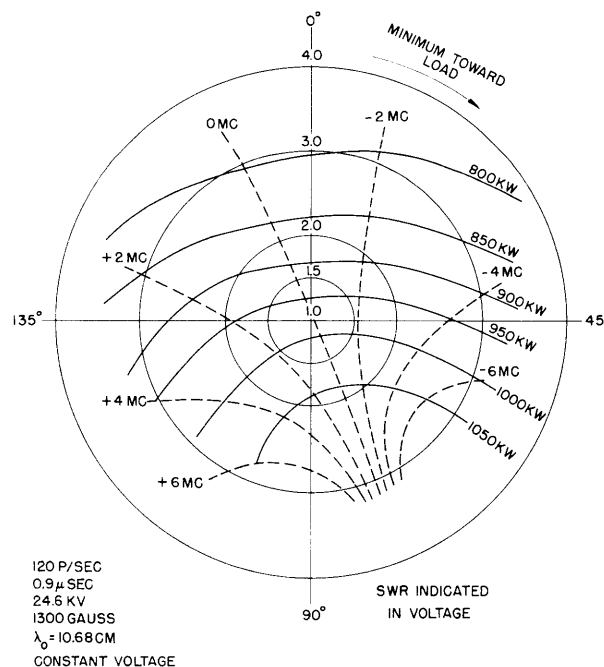


Fig. VIII-1

Rieke diagram for magnetron MF-14B.

(VIII. TUBE RESEARCH AND DEVELOPMENT)

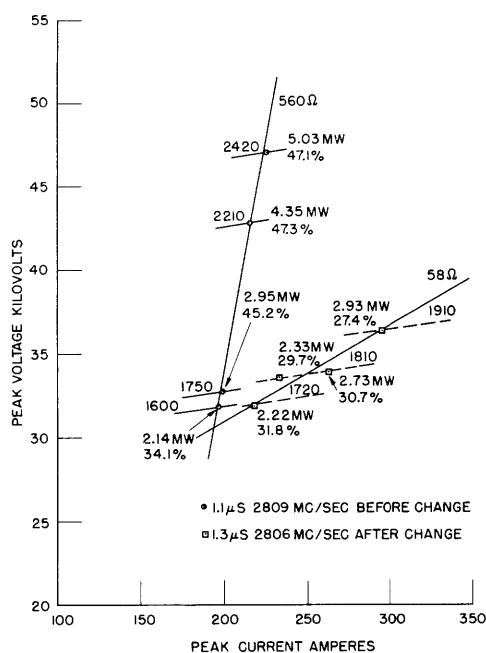


Fig. VIII-2

MF-14B performance chart. Magnetic-field values shown are in gauss. Repetition rate 120 pps 3:1 ratio pulse transformer.

a 1-μsec pulse.

The pulse transformer was changed to the 3:1 ratio, 20-Mw unit built especially for the project, and the following maximum performance data were observed:

| | |
|-----------------|--------------|
| Peak output | 5.0 Mw |
| Peak input | 10.6 Mw |
| Efficiency | 47.5 percent |
| Pulse length | 1.1 μsec |
| Repetition rate | 120 pps |
| Peak voltage | 47.1 kv |
| Peak current | 225 amp |
| Magnetic field | 2420 gauss. |

Operation at this power level was accompanied by severe internal sparking with current flowing as long as 10 μsec for many successive individual pulses. The sparking continued to increase in intensity after reaching this maximum power level, and subsequent operation of the tube was marked by a sharp decline in output, a shift in the magnetic field requirements, and a change in dynamic impedance as indicated in the incomplete performance chart shown in Fig. VIII-2. Only a few points were secured

vacuum tight. The dc primary emission from the cathode was very low (approximately 7 ma/cm² at 600 volts and normal heater power of 200 watts). Such poor cathode performance is believed primarily due to processing conditions rather than to the cooling effect of the large end shields, since the current density increased to only 20 ma/cm² at 600 volts and a heater power of 275 watts.

Despite its low-emission cathode, magnetron MF-14B performed well on the test bench. By using a 2.25:1 ratio, 10-Mw pulse transformer originally designed for the HP-10V magnetron, peak power outputs of 2.5 Mw to more than 4 Mw were obtained at 40 percent efficiency with a 1-μsec pulse. With a 5-μsec pulse the tube delivered 1-Mw peak and 650 watts average power at 50 percent efficiency. Output and efficiency were limited by what appeared to be an internal parasitic oscillation involving the cathode and cathode lead structure. Figure VIII-1 shows a Rieke diagram taken at a low power level with

(VIII. TUBE RESEARCH AND DEVELOPMENT)

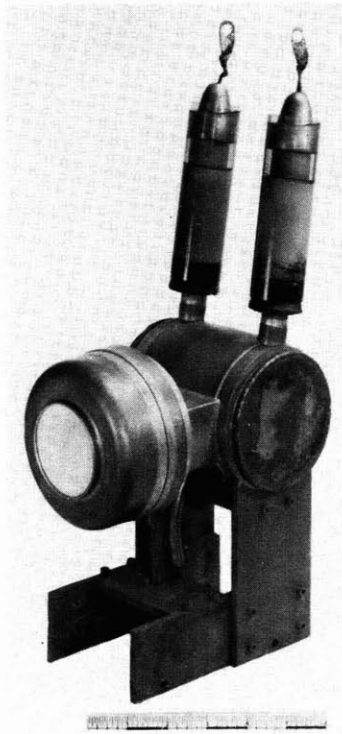


Fig. VIII-3
MF-14B magnetron.

because of the sudden change in the magnetron. In addition to sparking, the tendency to misfire and become unstable also increased as the power output decreased.

Accordingly, magnetron MF-14B was removed from the test bench after a total operating time of 32.6 hours. Figure VIII-3 is a photograph of the tube with its high voltage connectors attached. A resonance curve was taken which disclosed a large decrease in the unloaded Q of the magnetron while there was no significant change in the loaded Q .

In order to account for these changes in performance and characteristics, the magnetron was cut apart for examination. The cathode was severely pitted, and powdered nickel on the surface was vaporized by sparking at the 5-Mw level. Figure VIII-4 shows part of the surface area which was opposite the output slot upon which copper was sputtered from hot spots on the adjacent vane tips. The brighter spots in the picture are due to reflections from the nickel mesh exposed by the sparking.

The interior surfaces of the anode block were discolored by sparking and vaporization of the nickel powder. The end surfaces of the laminations showed signs of heavy sparking. The output circuit surfaces remained

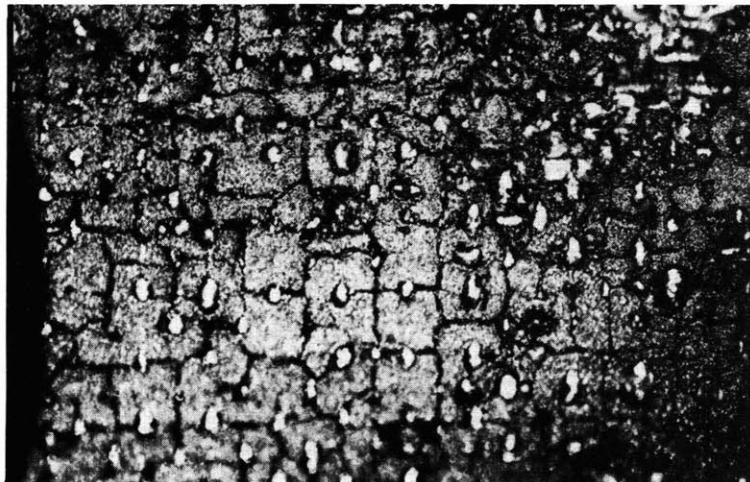


Fig. VIII-4
Photomicrograph of cathode surface
magnified ten times.

(VIII. TUBE RESEARCH AND DEVELOPMENT)

uncontaminated except for a dark band across the inner surface of the ceramic window parallel to and opposite the output slot. No conductance could be measured from end to end of the band even though it appeared to be composed of nickel.

The results obtained from magnetron MF-14B indicate that its performance was limited by the cathode. Hence, it is entirely conceivable that a magnetron provided with a more rugged cathode, such as the sintered molybdenum-thoria type, and designed to eliminate spurious resonances will produce substantially more pulse power at S-band.

Research Laboratory of Electronics Technical Report No. 242 will summarize the now complete experimental work on this project.

(VIII. TUBE RESEARCH AND DEVELOPMENT)

B. MICROWAVE TUBES

| | | |
|-----------------|-------------------|------------------|
| L. D. Smullin | A. W. Boekelheide | C. E. Muehe, Jr. |
| Prof. L. J. Chu | B. Epsztein | H. E. Rowe |
| E. J. Baghdady | C. Fried | C. R. Russell |
| A. D. Berk | H. A. Haus | L. Stark |

1. Noise and Space-Charge Waves

a. A multivelocity electron beam in a cylindrical drift tube

An attempt has been made to explain the experimentally observed variation of the standing-wave ratio of noise waves in a drift tube with a longitudinal magnetic field. The theoretical formula for the standing-wave ratio in the presence of a velocity spread as reported on page 42 of the Quarterly Progress Report, April 15, 1952, has been applied. The following assumptions are made:

(a) The beam is completely neutralized.

(b) The electrons entering the magnetic field obtain a transverse velocity according to Busch's theorem at the expense of their longitudinal velocity. Thus, a velocity spread is introduced which is a function of the magnetic field.

(c) The effect of the velocity spread can be treated by an infinite parallel-plane analysis by introducing the usual correction factor for the plasma frequency.

The equations for the fractional velocity spread α/W and the standing-wave ratio are:

$$\frac{\alpha}{W} = \frac{\eta(r_1 B)^2}{16V_0}$$
$$SWR = 12 \left(\frac{W}{\alpha} \Gamma \frac{\omega_p}{\omega} \right)^2$$

where

η is the charge-to-mass ratio of the electron

r_1 is the maximum radius of the beam

B is the magnetic field

ω_p/ω is the ratio of plasma frequency to operating frequency

V_0 is the voltage of the beam.

In plotting the "theoretical curve" in Fig. VIII-5, the experimental values for the plasma wavelength, and Γ^2 are inserted into the theoretical formula. The space-charge smoothing factor Γ^2 expresses the ratio of the maximum mean-square noise current fluctuations $2eI_0 \Delta f \Gamma^2$ to pure shot noise fluctuations $2eI_0 \Delta f$.

It can be seen from the figure which represents a typical plot of one of several experiments that there is no agreement between this simple theory and experiment in the

(VIII. TUBE RESEARCH AND DEVELOPMENT)

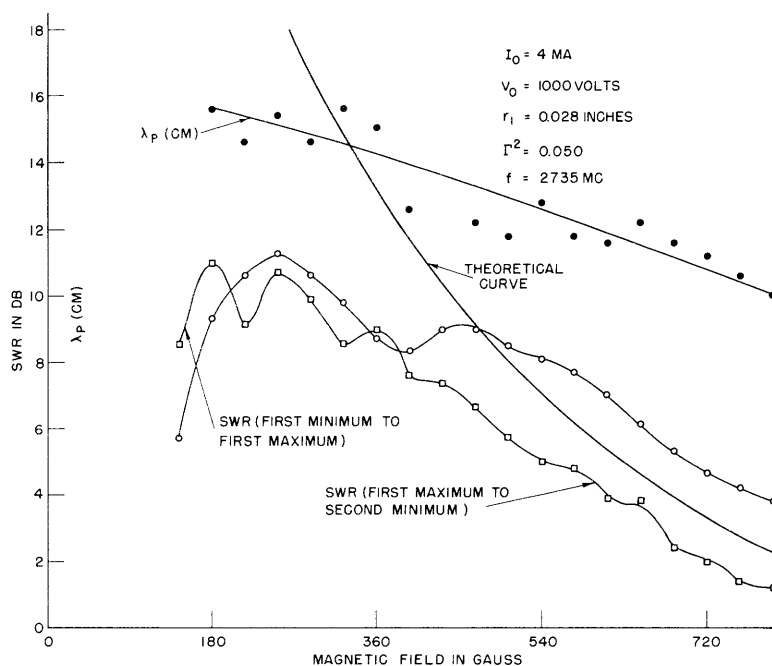


Fig. VIII-5
Standing-wave ratio vs magnetic field.

region of low magnetic fields. The agreement becomes quite good at large magnetic fields. It seems reasonable to consider the velocity spread due to the magnetic field to be responsible for the reduction of the standing-wave ratio at values of the magnetic field approximately two and a half to three times Brillouin field.

A similar experiment in which the gun was situated in the magnetic field showed no influence of the magnetic field upon the standing-wave ratio. In this case the electrons all make similar spirals about their individual orbits, so that no velocity spread is introduced by the magnetic field.

The experimental work of C. E. Muehe, Jr. has been written as a Master's Thesis for the Department of Electrical Engineering and will appear shortly as a Research Laboratory of Electronics technical report.

C. E. Muehe, Jr., H. A. Haus

b. Calculation of noise in a finite diameter beam

This work is being prepared as a Doctoral thesis for the Department of Electrical Engineering.

H. E. Rowe

(VIII. TUBE RESEARCH AND DEVELOPMENT)

2. Traveling-Wave Amplifiers

a. Double helices

A bifilar helix has been built for the pulsed, 3-cm, 10-kv, traveling-wave amplifier. No difficulty was experienced in matching it to the coupling waveguides.

A demountable system is being assembled for testing pulsed tubes of this type.

E. J. Baghdady, C. R. Russell

3. 1-Mev Pulsed Electron Source

This work has been summarized in a Master's Thesis for the Department of Electrical Engineering, and in a Research Laboratory of Electronics technical report which will appear shortly.

A. W. Boekelheide

4. Internally Coated Cathodes

A series of preliminary experiments has been conducted on a new type of cathode. In the present experiments two different configurations have been used. In Fig. VIII-6a the inside of the cathode cup was all oxide-coated, and current was drawn through a 0.0135-inch diameter hole to an anode 0.1-inch away. One theory of the operation of this cathode is that the interior of the cup contains a neutral electron gas, produced by virtue of the positive ions known to be emitted from oxide cathodes. Another theory assumes that current is only drawn from the ring of coating immediately adjacent to the hole. The cathode shown in Fig. VIII-6b should not produce an electron gas, since only the top is coated.

Figure VIII-7 shows the current-voltage characteristics as a function of brightness temperature for the cathode shown in Fig. VIII-6a. Currents up to 60 ma were drawn, with densities up to 60 amp/cm². The tube never obeys Child's Law ($I \sim V^{3/2}$). There is never a true temperature-limited region nor a space-charge-limited region of operation. Figure VIII-8 shows the noise-reducing properties (Γ^2) of the cathode, measured at about 2 Mc/sec and at various cathode temperatures. The minima were real and reproducible. We note that the least value of Γ^2 is lower than is commonly reported for conventional cathodes.

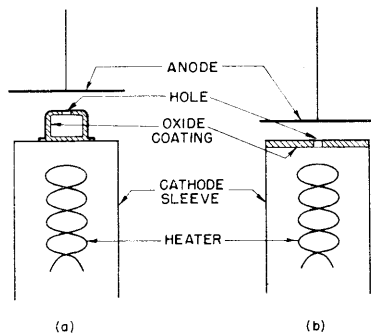


Fig. VIII-6
Internally coated cathodes.

In order to check the electron gas theory, a strong axial magnetic field was applied to the cathode. With large anode voltages, no change in current was caused

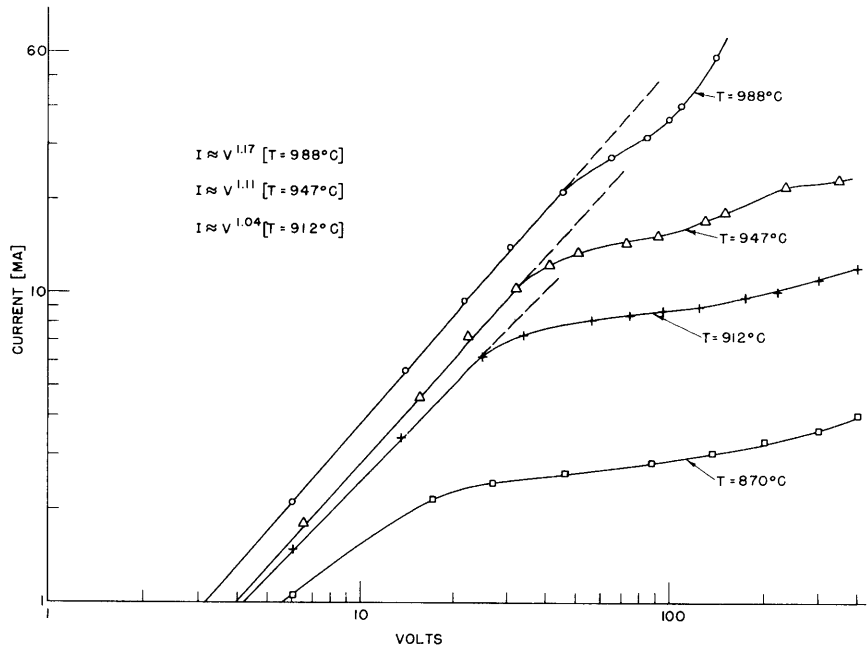


Fig. VIII-7
Voltage current characteristics.

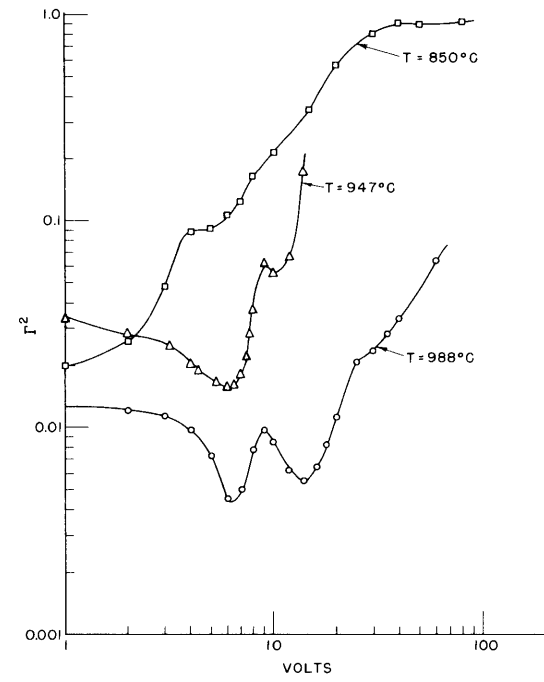


Fig. VIII-8
Ratio of noise power to shot noise vs voltage. (Frequency = 2.45 Mc/sec.)

(VIII. TUBE RESEARCH AND DEVELOPMENT)

by the field. At low voltages (<10 volts), reductions of about 20 percent in current were observed. It was postulated that the field would prevent current from the side walls from reaching the hole if the cathode emission occurred as an electron gas. The negative results of this test led to the construction of the cathode shown in Fig. VIII-6b. Here, only the inside of the top surface was coated and the heater was inside the cathode proper. This tube gave substantially the same current as the first so that it now appears that emission is from the edge of the hole rather than from a gas. The very large current densities are tentatively explained by the fact that the coating is shielded from the anode and therefore escapes contamination from that source.

A number of hysteresis phenomena have been observed, both long and short time-constant. Further tests will be made on multiple-hole cathodes and radially emitting cylindrical cathodes.

L. D. Smullin, B. Epsztein, C. Fried

5. The Use of Ferrites at Microwave Frequencies

a. Impedance of a cavity containing a generalized medium

The investigation of the input and transfer impedances of a two-input cavity containing a generalized medium has been extended to include the case for which both σ and μ are tensor quantities. (See Quarterly Progress Report, July 15, 1952, pp. 60-63, for a precise formulation of the problem.) The method followed is that given by Slater (ref. 1). It has been necessary, however, to extend it by introducing magnetic currents in order to include the effect of inhomogeneity in the magnetic susceptibility within the cavity. In this general case the impedance matrix

$$Z = \begin{bmatrix} Z_{11} & Z_{12} \\ Z_{21} & Z_{22} \end{bmatrix}$$

is given by

$$Z_{11} = v_{a1}^2 \frac{K_{\beta}(1 + J_{aa}) - \Lambda_{\beta} J_{a\beta} \frac{k_{\beta}}{k_a}}{\Delta} \quad (1)$$

$$Z_{12} = v_{a1} v_{\beta 2} \frac{K_{\beta} J_{\beta a} \frac{k_a}{k_{\beta}} - \Lambda_{\beta}(1 + J_{\beta\beta})}{\Delta} \quad (2)$$

$$Z_{21} = v_{\alpha 1} v_{\beta 2} \frac{K_{\alpha} \frac{k_{\beta}}{k_{\alpha}} J_{\alpha\beta} - \Lambda_{\alpha} (1 + J_{\alpha\alpha})}{\Delta} \quad (3)$$

$$Z_{22} = v_{\beta 2}^2 \frac{K_{\alpha} (1 + J_{\beta\beta}) - \Lambda_{\alpha} \frac{k_{\alpha}}{k_{\beta}} J_{\beta\alpha}}{\Delta} \quad (4)$$

where

$$J_{\alpha\beta} = \int_{\text{vol.}} \vec{H}_{\alpha} \cdot \vec{\chi}_{\text{m}} \cdot \vec{H}_{\beta} dv \text{ with analogous meanings for } J_{\alpha\alpha}, J_{\beta\alpha} \text{ and } J_{\beta\beta}$$

$\vec{\chi}_{\text{m}}$ = magnetic susceptibility tensor

$$K_{\alpha} = \frac{k_{\alpha}^2 - k^2(1 + J_{\alpha\alpha})}{jkc\mu_0} + I_{\alpha\alpha}(1 + J_{\alpha\alpha}) + \frac{k_{\alpha}}{k_{\beta}} I_{\alpha\beta} J_{\beta\alpha}$$

$$\Lambda_{\alpha} = (jkc\epsilon_0 + I_{\alpha\alpha}) \frac{k_{\beta}}{k_{\alpha}} I_{\alpha\beta} + I_{\alpha\beta}(1 + J_{\beta\beta}).$$

K_{β} and Λ_{β} are obtained by interchanging α and β in the expression for K_{α} and Λ_{α} , respectively. Finally, $\Delta = K_{\alpha}K_{\beta} - \Lambda_{\beta}\Lambda_{\alpha}$. The rest of the symbols have the same meaning as those in reference 2.

For a single input ($v_{\beta 2} = 0$) the driving-point impedance of the cavity becomes

$$Z_{\text{in}} = Z_{11}. \quad (5)$$

Note that the expressions for driving-point and transfer impedances given in reference 2 are special cases of the preceding expressions and may be obtained from the latter by putting $\chi_{\text{m}} = 0$.

A case of particular interest is that of ferrites. The previous expressions simplify considerably if this medium (the ferrite) is placed in a region of vanishing electric field and intense magnetic field. Then all four integrals of the type $I_{\alpha\beta}$ (see ref. 2) become vanishingly small and can be neglected.

As an illustration consider a cylindrical cavity with a small piece of ferrite at the center of one of the faces, and a steady magnetic field along the axis of the cylinder. Here α and β represent the two degenerate TE_{111} modes (in space quadrature). For this particular case the input impedance (Eq. 5) becomes

$$Z = jkc\mu_0 v_{\alpha 1}^2 \frac{\left[k_{\alpha}^2 - k^2(1 + \tau\chi\phi^2) \right] (1 + \tau\chi\phi^2) + (k\tau\kappa\phi^2)^2}{\left[k_{\alpha}^2 - k^2(1 + \tau\chi\phi^2) \right]^2 - (\tau\kappa k^2\phi^2)^2}$$

(VIII. TUBE RESEARCH AND DEVELOPMENT)

where τ = volume of ferrite

ϕ = a numerical factor depending on the dimensions of the cavity

and χ and κ are defined by the expression for the magnetic susceptibility tensor

$$\chi_m = \begin{bmatrix} \chi & -j\kappa & 0 \\ j\kappa & \chi & 0 \\ 0 & 0 & 0 \end{bmatrix}$$

and they are both functions of the frequency.

A. D. Berk, B. Lax (Lincoln Laboratory)

References

1. J. C. Slater: Microwave Electronics, Van Nostrand, 1950, Ch. IV
2. Quarterly Progress Report, Research Laboratory of Electronics, M. I. T. July 15, 1952, pp. 60-63